Journal of Magnetic Resonance 306 (2019) 128–133

Contents lists available at ScienceDirect

Journal of Magnetic Resonance

journal homepage: www.elsevier.com/locate/jmr

High frequency dynamic nuclear polarization: New directions for the 21st century

Robert G. Griffin [a,b,*], Timothy M. Swager [b], Richard J. Temkin [c]

[a] Francis Bitter Magnet Laboratory, Massachusetts Institute of Technology, Cambridge, MA 02139, United States
[b] Dept. of Chemistry, Massachusetts Institute of Technology, Cambridge, MA 02139, United States
[c] Plasma Science and Fusion Center and Dept. of Physics, Massachusetts Institute of Technology, Cambridge, MA 02139, United States

ARTICLE INFO

Article history:
Received 26 May 2019
Revised 3 June 2019
Accepted 8 July 2019
Available online 12 July 2019

Keywords:
Dynamic nuclear polarization
Polarizing agents
High frequency microwaves
Pulsed DNP

1. Introduction

Dynamic nuclear polarization (DNP) is a technique that permits the sensitivity of nuclear magnetic resonance (NMR) experiments to be enhanced by a factor of (γ_e/γ_n) where the γ's are the gyromagnetic ratios of the electron and a nuclear spin, respectively. When the nuclear spin is ^{1}H, then optimally $(\gamma_e/\gamma_H) \sim 660$. At present, $\varepsilon \sim 100$ is readily achieved but even this "modest" enhancement means that the experimental acquisition time is reduced by a factor of 10^4. *Thus, an experiment can be done in a single day that would otherwise require ~ 30 years of signal averaging.* Accordingly, the incorporation of DNP into MAS and solution experimental protocols has enabled many experiments that are otherwise simply not possible. Furthermore, DNP experiments are in principle quite straightforward to perform and involve introducing a paramagnetic polarizing agent such as a bisnitroxide biradical into a glassy matrix containing the solute molecule of interest. Subsequently, the sample is irradiated with high frequency microwaves that excite electron-nuclear spin transitions, and, via a number of mechanisms discussed below, the large polarization in the electron spin reservoir is transferred to the nuclei.

The renaissance that is occurring in the development of microwave driven DNP has brought the technique to a point where it is widely applicable to problems in a variety of fields -- biophysics, chemistry, materials science, imaging, etc. This renaissance was nucleated by magic angle spinning (MAS) experiments performed on polymers and other materials in the 1980s where the necessity of observing low-γ nuclei ^{13}C, ^{15}N, etc. in natural abundance limited the sensitivity of the experiment. In addition, the tantalizing possibility of determining the structure of membrane and amyloid proteins and other large biological systems was clearly possible via dipole recoupling [1–6], but also limited by sensitivity considerations. In order to address these problems, MAS-DNP technology was developed for experiments at 60 MHz ^{1}H frequencies (40 GHz for $g \sim 2$ electrons) to enhance sensitivity in ^{13}C spectra [7–11]. However, because of the limited frequency range of available klystron microwave (μw) sources [12], these experiments were constrained to low magnetic fields.

Concurrent with the publication of these results, the field of NMR was transitioning to high field superconducting magnets operating first at ~5 T and today up to 23.5 T with higher fields (30–35 T) on the horizon. Thus, if DNP were to be more than an intellectual curiosity, then it would be essential to develop μw sources capable of generating watts of power in the frequency range ~100–1000 GHz to mate with these high fields. Although there are several sources that can produce radiation in this regime, the only source capable of routinely delivering 10–100 W of power is the gyrotron. In particular, the gyrotron is a form of electron cyclotron maser that uses a simple tapered cylindrical cavity as the resonant structure. The cavities are overmoded, typically several wavelengths in diameter, and these dimensions and the field

* Corresponding author.
E-mail address: rgg@mit.edu (R.G. Griffin).

https://doi.org/10.1016/j.jmr.2019.07.019
1090-7807/

strength of the magnet at cyclotron resonance determine the operating frequency. Furthermore, the cavity design allows gyrotrons to operate at high average power at sub-terahertz and terahertz frequencies. Because of the possibility of this scalable technology, we began to develop these devices for DNP applications in the mid 90s [13,14], and a photograph of our original 140 GHz system is shown in Fig. 1. Fortunately, our early prognosis as to the applicability of gyrotrons for high frequency DNP was correct, and there are now about 50 gyrotron based DNP spectrometers worldwide. Most of these are based on commercial instrumentation, now available from Bruker and operating at 400 MHz/263 GHz; but there are a substantial number of instruments at 600 MHz/395 GHz and 800 MHz/527 GHz and a single 900 MHz/593 GHz spectrometer. In addition, a number of home-built spectrometers are in operation.

In 1812 Sir Humphrey Davey [15] stated that "Nothing promotes the advancement of science so much as a new instrument". This elderly adage is particularly applicable to the future of DNP, as the future of the field depends strongly on the availability new instrumentation – microwave sources, low temperature probes, high spinning frequency rotors, etc. -- as well as new polarizing agents. We now discuss some of these possibilities and how they might affect the future directions of dynamic nuclear polarization.

2. Polarizing agents

All DNP experiments require a source of polarization and early efforts employed monoradicals such as nitroxides [16], BDPA [17] (Fig. 2(a–c)) and metals such as Cr(V) [18]. In 2004 we realized that the three spin cross effect (CE) could be mediated more effectively by increasing the e^--e^- dipole coupling by tethering two TEMPO radicals [19]. This improved enhancements by a factor of 3–4 over TEMPO and stimulated the development of a large series of bis-nitroxides for DNP in both aqueous and organic solvents. The first successful polarizing agent for aqueous media was TOTAPOL (Fig. 2 (d)) with a 21 MHz e^--e^- coupling[20,21] and thereafter AMUPol (Fig. 2(e)) [22] was developed which is the current favorite for experiments in d_8-glycerol/90% D_2O/10% H_2O solutions (a.k.a. "DNP juice") at 400 and 600 MHz. A typical nitroxide EPR spectrum and field profile are shown in Fig. 3. AMUPol's success is due to its short urea linker and larger (35 MHz) e^--e^- coupling, a PEG group to improve solubility, and the replacement of the —CH_3 groups on the TEMPO moieties by tetrahydropyran rings to lengthen the T_{1e} and improve the enhancements. On/off enhancements of up to

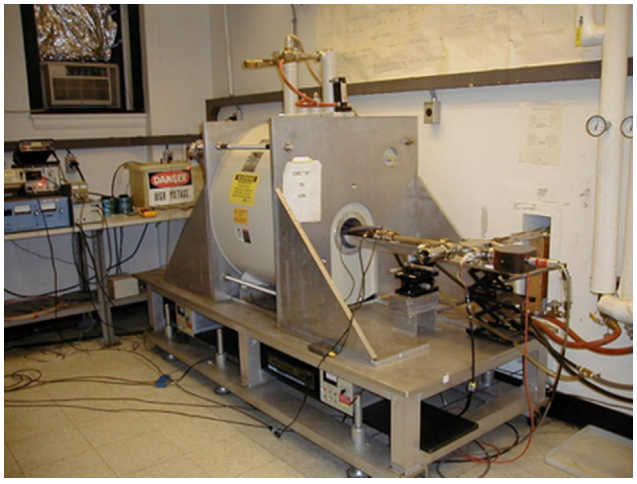

Fig. 1. Original 140 GHz gyrotron oscillator use for DNP experiments at 211 MHz ^{1}H frequencies.

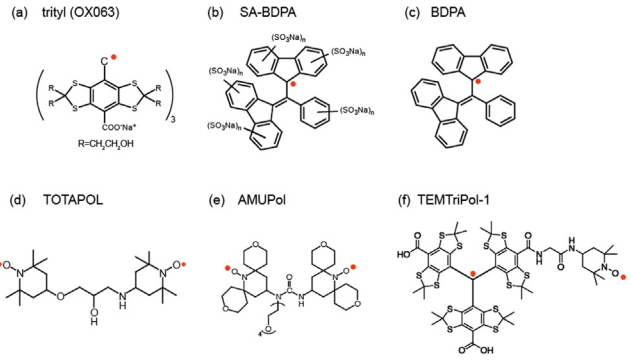

Fig. 2. Molecular structures of polarizing agents for SE, OE and CE DNP. (top) Narrow line radicals (trityl, SA-BDPA and BDPA) that support the SE and OE. (bottom) bis-nitroxides that mediate the CE. TEMTriPol-1 is a mixed radical that performs well at high field and is not subject to depolarization.

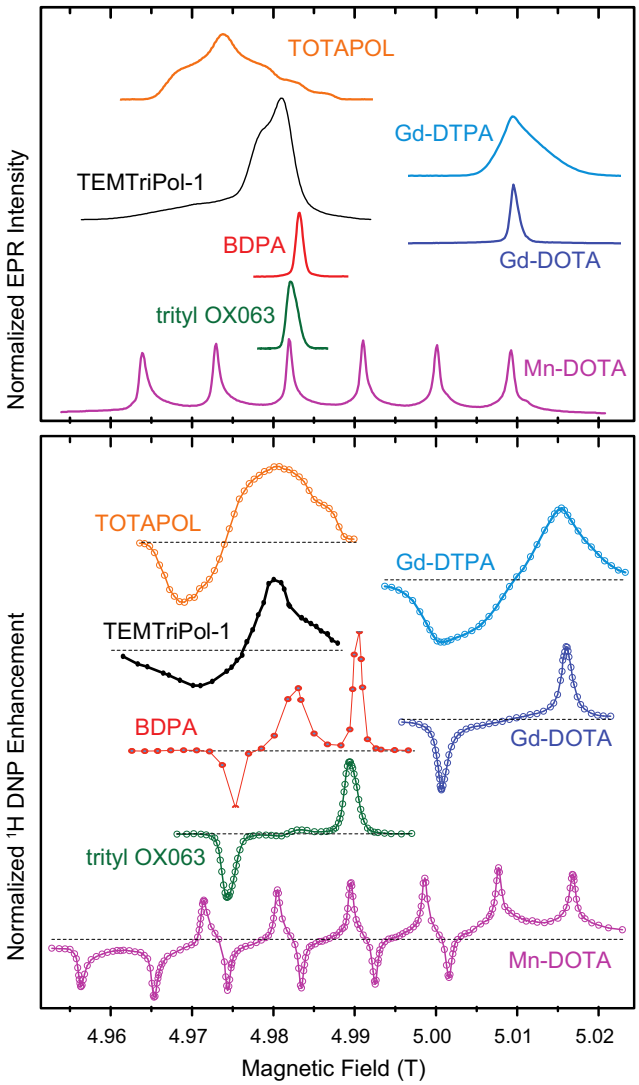

Fig. 3. (top) 140 GHz EPR spectra and (bottom) 211 MHz Zeeman field profiles for TOTAPOL, BDPA, trityl and TEMTriPol-1 and some Gd^{3+} and Mn^{2+} DOTA and DTPA complexes. The field profiles illustrate those expected for the CE (TOTAPOL and TEMriPol-1) the Overhauser effect (BDPA) and the SE (OX063, Mn^{2+} and Gd^{3+} and BDPA). This figure is an updated version of a figure prepared originally by B. Corzilius.

400 have been observed with AMUPol [23]. The large TEKPol series was developed for DNP in non-aqueous media [24] and has been very successful for DNP experiments involving materials science and surfaces [25].

Despite their success, the bis-nitroxides used in CE experiments exhibit two problems. The first is depolarization which arises because of the level crossing that occurs when the sample is rotated in a MAS experiment [26,27] which leads to a factor of ~2 loss in signal intensity. In addition, the enhancements scale down at higher frequencies such as 800 MHz. In 2007 we suggested tethering a narrow line radical (trityl or BDPA) to TEMPO to increase the enhancements and reported initial results with physical mixtures of radicals of trityl and TEMPO [28] and subsequently we prepared a BDPA-TEMPO, although it was not used for DNP experiments [29]. More recently, trityl-TEMPO biradicals became available and were shown to function well even at 800 MHz/527 GHz in aqueous media [30] and a BDPA-TEMPO was used successfully at high field and high spinning frequency, $\omega_r/2\pi = 40$ kHz [31]. An EPR spectrum and field profile of TEMTriPol-1 are included in Fig. 3. The advantage of these radicals is that they do not depolarize and perform well at fields up to 18.8 T and at high spinning frequencies. Continuing synthetic efforts to produce stable, soluble, efficient mixed radical polarizing agents are essential for advancing the field.

Narrow line radicals like trityl and BDPA mediate the solid effect (SE) and Overhauser effect (OE) with peaks in the Zeeman field profile at $\omega_{0S} \pm \omega_{0I}$ as shown in Fig. 3. Although the theory of the SE has recently been reformulated in detail [32,33], it is not widely used in applications since the enhancements scale as $(\omega_{1S}/\omega_{0I})^2$. As we increase ω_{0I} the enhancements are low, and furthermore, the cross effect yields larger enhancements. However, as the sample sizes decrease and we become more efficient at generating larger Rabi fields, the SE could become a competitive approach, since ε also scales $(\omega_{1S})^2$. To date little effort has been expended on increasing the Rabi fields.

Developing polarization agents with metal ions is still at an early stage and some results for Gd^{3+} and Mn^{2+}, two honorary $g \sim 2$ metal ions, are illustrated in Fig. 3. Both show SE profiles and the multiplicity of lines in the Mn^{2+} spectrum is due to the I = 5/2 nuclear spin.

One final comment concerns the OE which requires a narrow line radical. The OE in insulators was initially observed with SA-BDPA [34] in "DNP juice" and subsequently with BDPA in organic matrices [35–37]. A field profile with an enhancement at the EPR frequency is illustrated in Fig. 3 for BDPA in ortho-terphenyl. Two advantages of the OE are that it scales with $\omega_{0I}/2\pi$ and is not subject to depolarization effects. However, at the moment the mechanism underlying the OE is not understood, and we have only one radical, BDPA, which supports the OE mechanism. This is an area ripe for future developments.

3. Millimeter wave microwave sources for DNP

3.1. Solid state and klystron microwave sources

Stable μw sources are a requisite for successful DNP, and a gyrotron was chosen for the initial high frequency experiments for reasons outlined above. However, at what are today low μw frequencies - i.e., ≤263 GHz -- there are now two alternative sources that will suffice to produce reasonable enhancements; namely, solid state diodes and extended interaction klystrons (EIK's). Although Gunn and Impatt diodes were used in early DNP experiments [38], their power output was limited to ~20 mW, and thus their use was quickly superseded by the gyrotron. However, improvements in solid state technology have raised the power levels to ~250 mW at 263 GHz using solid state sources and an amplifier/multiplier chain, and recently these improved sources were successfully used to obtain enhancements of ~100 in model systems [39].

A 140 GHz EIK was also used in the earliest DNP experiments from our laboratory [40], and, like solid state devices, the EIK's have also continued to advance. At present there are robust EIK's available at W-band, 95 GHz, and they currently can produce a few watts of power at 263 GHz [41]. As these devices improve, they will also become candidates for incorporation into commercial and homebuilt DNP spectrometers.

At present DNP experiments with both solid-state sources and klystrons are limited to ≤263 GHz and lower frequencies, because the power outputs and lifetimes of the devices at higher frequencies drop significantly. In the case of EIK's, the size of the slow wave structure decreases with decreasing wavelength, and the smaller size structures are more susceptible to damage by a stray electron beam or can overheat. Likewise, because of the reduced dimensions, power dissipation for solid state devices becomes an issue. Thus, for the immediate future DNP experiments at 395 GHz/600 MHz and above will likely require gyrotrons. In the longer term, there is great interest in both the solid state [42,43] and vacuum electronic device [44] communities in advancing to higher frequencies.

3.2. Tunable gyrotrons

The types of experiments and polarizing agents that are useful for a broad range of DNP applications are now well defined. In turn the EPR spectrum of the polarizing agent determines features of the μw sources that are required for DNP and stipulates how they may change in the future. For example, the cross effect (CE) mechanism uses nitroxides, such as TOTAPOL, AMUPol, TEKPol or mixed radicals, whereas the solid effect (SE) is supported by the two monoradicals BDPA or trityl, and the Overhauser effect (OE) only by BDPA. These molecular structures are illustrated in Fig. 2, and their EPR spectra and Zeeman field profiles are illustrated in Fig. 3. Since the g-values of these radicals differ, it is necessary to irradiate with μw's of different frequencies, or to sweep the magnetic field if the μw source is not tunable. Currently, it is customary to use NMR magnets with superconducting sweep coils that is now a standard commercial product. However, since sweeping the field generally perturbs the homogeneity, it is desirable to consider sources with tunable μw frequencies.

Currently, most gyrotrons used for DNP are fixed frequency oscillators, but, it is possible to construct a tunable gyrotron and this has been done at 250, 330 and 460 GHz. Briefly, this is accomplished by lengthening the gyrotron cavity so that it supports additional longitudinal modes. For example, our 250 GHz fundamental gyrotron operates in a $TE_{5,2,q}$ mode and with an extended cavity can access longitudinal modes with q = 1–5 which permits tuning over 3 GHz [45]. A similar approach was used in second harmonic gyrotrons [46–48] operating at 330 and 460 GHz. At 460 GHz the gyrotron was operating in $TE_{11,2,q}$ mode and with q = 2, 3 or 4 enabled tuning over about 1 GHz as illustrated in Fig. 4. In this case the power output is flat at ~4 W from 460.2 to 461.1 GHz as the gyrotron field was swept from 8.43 to 8.47 T. Tuning by varying the gyrotron operating voltage is also possible.

As mentioned above, the advantage to sweeping the gyrotron frequency rather than the NMR magnet field is that the homogeneity of the NMR field is not perturbed. If the NMR magnet has a Z_2 shim, then the Z_0 sweep coil will couple strongly to Z_2 and extensive shimming is required to regain the homogeneity. However, since a Z_2 shim is not required for MAS experiments [49] the Bruker 18.8 T DNP magnets, which are used extensively for MAS experiments, do not have a such a shim. Furthermore, a tunable

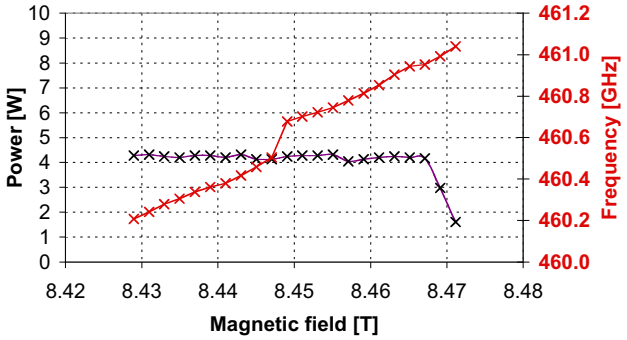

Fig. 4. Frequency tuning of the 460 GHz gyrotron over 800 MHz by varying the gyrotron magnetic field. Voltage tuning is also possible. The power output is constant at ~4 W, Higher powers are available at other voltage field settings.

gyrotron source will make it possible to perform DNP experiments on essentially any of the existing fixed field NMR magnets now in operation.

A second possibility for a tunable gyrotron was recently discussed by Barnes et al. [50] In particular, they demonstrated that the microwave frequency can be modulated by varying the anode voltage. This strategy results in more rapid frequency response than can be achieved by changing the potential of the electron emitter and does not require a custom triode electron gun. The 200 GHz gyrotron frequency was swept with a rate of 20 MHz/s over a 670 MHz bandwidth in a static magnetic field.

Thus, in the future we will likely see gyrotron oscillators that are tunable, albeit over a limited range, rather than using a fixed frequency oscillator and an NMR magnet with a sweep coil. We would expect that these tunable oscillators to be developed at frequencies up to at least 800 GHz corresponding to a 1.2 GHz ^{1}H frequency.

3.3. Gyroamplifiers

Another area where we will likely see new μw technology important for DNP is microwave amplifiers. In particular, gyroamplifiers are one of the few amplifier options operating in the millimeter wave regime [51]. The motivation for developing these devices is discussed below in the section on pulsed DNP, but, like RF amplifiers in conventional NMR instruments, they should permit modulation of the phase, frequency and amplitude of microwave pulses. In turn, this should enable the development of new

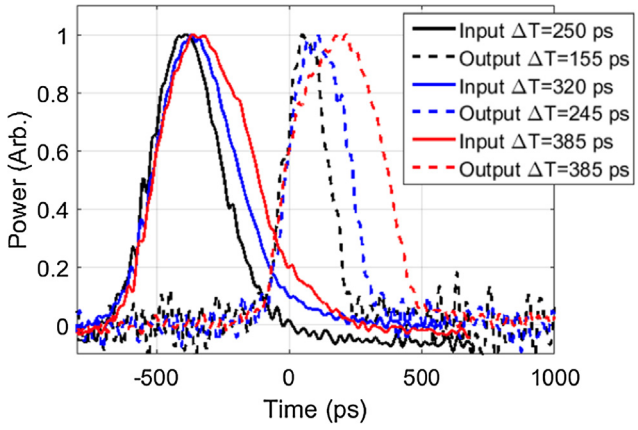

Fig. 5. Input and output pulses from the 250 GHz gyroamplifier. The pulse widths varied from 250 to 385 ps input and the output from 155 to 385.

approaches to polarization transfer which are not field dependent as is the case with the SE and CE.

In our group we have constructed gyroamplifiers operating at 140 [52] and 250 GHz [53,54] specifically for applications to DNP. The 250 GHz amplifier utilizes a photonic band gap resonator. As illustrated in Fig. 5 the device has generated pulses of ~100–400 ps duration and has an 8 GHz bandwidth and 38 dB gain. With input drive from a diode of 100–200 mW, the amplifier should yield 600–1200 W of output power and enable us to satisfy the NOVEL condition, $\omega_{0I} = \omega_{1S}$, at 380 MHz/250 GHz. As soon as amplifiers are successfully deployed for ~9 T fields there will undoubtedly be insatiable demand for higher frequencies.

4. Probes

Probes for DNP experiments are also undergoing significant evolution that will likely continue in the future in at least three areas. First, the 3.2 mm rotor, which is currently the default rotor diameter, will be replaced with 1.3 mm and smaller rotors. These will enable higher spinning frequencies and recently published data indicates that this could significantly improve the resolution in low temperature spectra [55]. Published reports indicate that at low temperature the broadening in the spectra is homogeneous [56] and this is removed by higher frequency spinning. In addition, the possibility of spinning at lower temperatures (~20–60 K) will increase enhancements [57] and, for economic reasons, has stimulated the construction of two closed cycle systems that use He as the driving fluid [58–60]. In addition, it is well known that the speed of sound in He gas is a factor of 3 higher than in N_2, and therefore higher spinning frequencies should be available with He recirculation systems. A third area where probes can be improved is the development of resonant structures for the microwave circuit. Initially the rotors used for DNP were 4.0 and 5.0 mm diameter and are too large to insert into a resonant structure without destroying the Q. However, as we transition to 1.3 and 0.7 mm and perhaps yet smaller rotors, we can start to design resonant structures with finite Q's. One approach involving a small waveguide and reflector on a 1.3 mm rotor has recently been published [61]. Another approach would be to employ TE_{011} type resonators that are used in high frequency EPR experiments [38] which could easily accommodate 0.7 mm rotors. Finally, spherical, rather than cylindrical, rotors were recently described [62,63]. Although they are at an early stage of development they offer certain advantages such as ease of sample irradiation and sample changing. With He gas a spinning frequency up to ~30 kHz was achieved.

5. Pulsed DNP at high magnetic fields

The history of magnetic resonance tells us that there are many advantages to performing time domain or pulsed rather than CW experiments. An early but relevant example are the ^{13}C solution experiments on proteins where CW heteronuclear (^{1}H-^{13}C) Overhauser effects were used to enhance signals by ~3. However, at $\omega_{0H}/2\pi > 60$ MHz the NOE's start to decrease rapidly, and *this lead to the interesting prediction that ^{13}C protein NMR should not be performed at fields higher than 1.5 T* [64]. The fact that CW heteronuclear NOE's were decreasing rapidly was correct, but this problem was solved with the introduction of pulsed transfer schemes, in particular INEPT [65], which is field independent. DNP is similar in that all of the CW mechanisms – the CE, SE and OE – are dependent on having the correct relaxation times to function properly and the enhancements scale weakly or inversely as $\omega_{0H}/2\pi$. Thus, if it were possible to perform pulsed DNP experiments, then they would in principle be magnetic field independent. In addition, the ability to manipulate the phase, amplitude and fre-

quency of the μw fields will likely stimulate the development of multiple new approaches to perform DNP as has been the case with pulsed NMR.

Stimulated by these ideas, we have performed a number of pulsed DNP experiments based on the original work by Wenckebach [66–70]; namely, NOVEL [71,72], ramped NOVEL [73], off-resonance NOVEL [74] and the frequency swept integrated solid effect (FS-ISE) [75]. These experiments have revealed a number of new features and a new mechanism, the stretched solid effect [76]. In addition, we recently published a new approach in the form of ***T***ime ***O***ptimized ***P***ulsed DNP (TOP DNP) where we were able to obtain enhancements comparable to NOVEL [77]. The approach utilizes a train of short pulses with timings and effective fields such that their frequency spectrum matches the nuclear Larmor frequency. To date all of these experiments have been performed at low frequencies (9, 34 and 95 GHz) where the technology is available to perform pulsed μw experiments. These results suggest an exciting number of possibilities for new approaches for DNP, and it will be interesting to see how they perform at higher frequencies with gyroamplifiers or other technology [78]. The DNP community is already aware of the advantages of time domain experiments, and as soon as the instrumentation is available there will be active research in this area.

Acknowledgements

The authors would like to express our sincere thanks to our many colleagues who have participated in the development of the instrumentation, of the DNP methods, and of the molecules that serve as polarizing agents mentioned in the text above. This research was supported by the NIH through grants to RGG (GM132079, GM132997), TMS (GM095843) and RJT (EB001965).

References

[1] J.M. Griffiths, R.G. Griffin, Nuclear-magnetic-resonance methods for measuring dipolar couplings in rotating solids, Anal. Chim. Acta 283 (1993) 1081–1101.
[2] A.E. Bennett, R.G. Griffin, S. Vega, Recoupling of homo- and heteronuclear dipolar interactions in rotating solids, NMR Bas. Princip. Prog. 33 (1994) 1–77.
[3] D.P. Raleigh, M.H. Levitt, R.G. Griffin, Rotational resonance in solid state NMR, Chem. Phys. Lett. 146 (1988) 71–76.
[4] M.H. Levitt, D.P. Raleigh, F. Creuzet, R.G. Griffin, Theory and simulations of homonuclear spin pair systems in rotating solids, J. Chem. Phys. 92 (1990) 6347–6364.
[5] A.E. Bennett, J.H. Ok, R.G. Griffin, S. Vega, Chemical-shift correlation spectroscopy in rotating solids - radio frequency-driven dipolar recoupling and longitudinal exchange, J. Chem. Phys. 96 (1992) 8624–8627.
[6] A.E. Bennett, C.M. Rienstra, J.M. Griffiths, W.G. Zhen, P.T. Lansbury, R.G. Griffin, Homonuclear radio frequency-driven recoupling in rotating solids, J. Chem. Phys. 108 (1998) 9463–9479.
[7] R.A. Wind, M.J. Duijvestijn, C. Vanderlugt, A. Manenschijn, J. Vriend, Applications of dynamic nuclear-polarization in C-13 Nmr in solids, Prog. Nucl. Magn. Reson. Spectrosc. 17 (1985) 33–67.
[8] D.J. Singel, H. Seidel, R.D. Kendrick, C.S. Yannoni, A spectrometer for EPR, DNP, and multinuclear high-resolution NMR, J. Magn. Reson. 81 (1989) 145–161.
[9] M. Afeworki, R.A. Mckay, J. Schaefer, Selective observation of the interface of heterogeneous polycarbonate polystyrene blends by dynamic nuclear-polarization C-13 Nmr-spectroscopy, Macromolecules 25 (1992) 4084–4091.
[10] M. Afeworki, J. Schaefer, Mechanism of DNP-enhanced polarization transfer across the interface of polycarbonate/polystyrene heterogeneous blends, Macromolecules 25 (1992) 4092–4096.
[11] M. Afeworki, J. Schaefer, Molecular dynamics of polycarbonate chains at the interface of polycarbonate/polystyrene heterogeneous blends, Macromolecules 25 (1992) 4097–4099.
[12] R.A. Wind, F.E. Anthonio, M.J. Duijvestijn, J. Smidt, J. Trommel, G.M.C.d. Vette, Experimental setup for enhanced 13C NMR spectroscopy in solids using dynamic nuclear polarization, J. Magn. Reson. 52 (1983) 424–434.
[13] L.R. Becerra, G.J. Gerfen, R.J. Temkin, D.J. Singel, R.G. Griffin, Dynamic nuclear polarization with a cyclotron resonance maser at 5 T, Phys. Rev. Lett. 71 (1993) 3561–3564.
[14] L.R. Becerra, G.J. Gerfen, B.F. Bellew, J.A. Bryant, D.A. Hall, S.J. Inati, R.T. Weber, S. Un, T.F. Prisner, A.E. McDermott, K.W. Fishbein, K.E. Kreischer, R.J. Temkin, D. J. Singel, R.G. Griffin, A spectrometer for dynamic nuclear-polarization and electron- paramagnetic-resonance at high-frequencies, J. Magn. Reson., Ser A 117 (1995) 28–40.
[15] S.H. Davey, Elements of Chemical Philosophy, 1812.
[16] G. Hartmann, D. Hubert, S. Mango, C.C. Morehouse, K. Plog, Proton polarization in alcohols at 50 kG, 1K, Nucl. Instrum. Meth. 106 (1973) 9–12.
[17] M. Borghini, W.D. Boer, K. Morimoto, Nuclear dynamic polarization by resolved solid-effect and thermal mixing with an electron spin-spin interaction reservoir, Phys. Lett. 48A (1974) 244–246.
[18] M. Krumpolc, J. Rocek, Synthesis of stable chromium(V) complexes of tertiary hydroxy acids, J. Am. Chem. Soc. 101 (1979) 1306–1309.
[19] K.N. Hu, H.H. Yu, T.M. Swager, R.G. Griffin, Dynamic nuclear polarization with biradicals, J. Am. Chem. Soc. 126 (2004) 10844–10845.
[20] C.S. Song, K.N. Hu, C.G. Joo, T.M. Swager, R.G. Griffin, TOTAPOL: a biradical polarizing agent for dynamic nuclear polarization experiments in aqueous media, J. Am. Chem. Soc. 128 (2006) 11385–11390.
[21] K.-N. Hu, C. Song, H.-H. Yu, T.M. Swager, R.G. Griffin, High-frequency dynamic nuclear polarization using biradicals: a multifrequency EPR lineshape analysis, J. Chem. Phys. 128 (2008) 052321.
[22] C. Sauvee, M. Rosay, G. Casano, F. Aussenac, R.T. Weber, O. Ouari, P. Tordo, Highly efficient, water-soluble polarizing agents for dynamic nuclear polarization at high frequency, Angewa. Chem.-Int. Ed. 52 (2013) 10858–10861.
[23] T.V. Can, Q.Z. Ni, R.G. Griffin, Mechanisms of dynamic nuclear polarization in insulating solids, J. Magn. Res. 253 (2015) 23–35.
[24] D.J. Kubicki, G. Casano, M. Schwarzwalder, S. Abel, C. Sauvee, K. Ganesan, M. Yulikov, A.J. Rossini, G. Jeschke, C. Coperet, A. Lesage, P. Tordo, O. Ouari, L. Emsley, Rational design of dinitroxide biradicals for efficient cross-effect dynamic nuclear polarization, Chem. Sci. 7 (2016) 550–558.
[25] A. Lesage, M. Lelli, D. Gajan, M.A. Caporini, V. Vitzthum, P. Miéville, J. Alauzun, A. Roussey, C. Thieuleux, A. Mehdi, G. Bodenhausen, C. Copéret, L. Emsley, Surface enhanced NMR spectroscopy by dynamic nuclear polarization, J. Am. Chem. Soc. 132 (2010) 15459–15461.
[26] K. Thurber, R. Tycko, Theory for cross effect dynamic nuclear polarization under magic angle spinning in solid state nuclear magnetic resonance: the importance of level crossings, J. Chem. Phys. 137 (2012), 084508–084501.
[27] F. Mentink-Vigier, S. Paul, D. Lee, A. Feintuch, S. Hediger, S. Vega, G. De Paepe, Nuclear depolarization and absolute sensitivity in magic-angle spinning cross effect dynamic nuclear polarization, PCCP 17 (2015) 21824–21836.
[28] K.-N. Hu, V.S. Bajaj, M.M. Rosay, R.G. Griffin, High frequency dynamic nuclear polarization using mixtures of TEMPO and trityl radicals, J. Chem. Phys. 126 (2007) 044512.
[29] E.L. Dane, T. Maly, G.T. Debelouchina, R.G. Griffin, T.M. Swager, Synthesis of a BDPA-TEMPO biradical, Org. Lett. 11 (2009) 1871–1874.
[30] G. Mathies, M.A. Caporini, V.K. Michaelis, Y.P. Liu, K.N. Hu, D. Mance, J.L. Zweier, M. Rosay, M. Baldus, R.G. Griffin, Efficient dynamic nuclear polarization at 800 MHz/527 GHz with trityl-nitroxide biradicals, Angewa. Chem.-Int. Ed. 54 (2015) 11770–11774.
[31] D. Wisser, G. Karthikeyan, A. Lund, G. Casano, H. Karoui, M. Yulikov, G. Menzildjian, A.C. Pinon, A. Purea, F. Engelke, S.R. Chaudhari, D. Kubicki, A.J. Rossini, I.B. Moroz, D. Gajan, C. Coperet, G. Jeschke, M. Lelli, L. Emsley, A. Lesage, O. Ouari, BDPA-nitroxide biradicals tailored for efficient dynamic nuclear polarization enhanced solid-state NMR at magnetic fields up to 21.1 T, J. Am. Chem. Soc. 140 (2018) 13340–13349.
[32] B. Corzilius, A.A. Smith, R.G. Griffin, Solid effect in magic angle spinning dynamic nuclear polarization, J. Chem. Phys. 137 (2012) 054201.
[33] A.A. Smith, B. Corzilius, O. Haze, T.M. Swager, R.G. Griffin, Observation of strongly forbidden solid effect dynamic nuclear polarization transitions via electron-electron double resonance detected NMR, J. Chem. Phys. 139 (2013) 6.
[34] O. Haze, B. Corzilius, A.A. Smith, R.G. Griffin, T.M. Swager, Water-soluble narrow-line radicals for dynamic nuclear polarization, J. Am. Chem. Soc. 134 (2012) 14287–14290.
[35] T.V. Can, M.A. Caporini, F. Mentink-Vigier, B. Corzilius, J.J. Walish, M. Rosay, W. E. Maas, S. Vega, T.M. Swager, R.G. Griffin, Overhauser effects in insulating solids, J. Chem Phys. 141 (2014) 064202.
[36] M. Lelli, S.R. Chaudhari, D. Gajan, G. Casano, A.J. Rossini, O. Ouari, P. Tordo, A. Lesage, L. Emsley, Solid-state dynamic nuclear polarization at 9.4 and 18.8 T from 100 K to room temperature, J. Am. Chem. Soc. 137 (2015) 14558–14561.
[37] S.R. Chaudhari, P. Berruyer, D. Gajan, C. Reiter, F. Engelke, D.L. Silverio, C.C. ret, M. Lelli, A. Lesage, L. Emsley, Dynamic nuclear polarization at 40 kHz magic angle spinning, PCCP 18 (2016) 10616.
[38] V. Weis, M. Bennati, M. Rosay, J.A. Bryant, R.G. Griffin, High-field DNP and ENDOR with a novel multiple-frequency resonance structure, J. Magn. Reson. 140 (1999) 293–299.
[39] I.V. Sergeyev, Fabien Aussenac, Armin Purea, Christian Reiter, Eric Bryerton, Steven Retzloff, Jeffrey Hesler, Leo Tometich, Melanie Rosay, Efficient 263 GHz magic angle spinning DNP at 100 K using solid-state diode sources, Solid State Nucl. Mag. 100 (2019) 63–69.
[40] S. Un, T. Prisner, R.T. Weber, M.J. Seaman, K.W. Fishbein, A.E. McDermott, D.J. Singel, R.G. Griffin, Pulsed dynamic nuclear-polarization at 5 T, Chem. Phys. Lett. 189 (1992) 54–59.
[41] K. Thurber, R. Tycko, Low-temperature dynamic nuclear polarization with helium-cooled samples and nitrogen-driven magic-angle spinning, J. Magn. Reson. 264 (2016) 99–106.
[42] J.V. Siles, K.B. Cooper, C. Lee, R.H. Lin, G. Chattopadhyay, I. Mehdi, A new generation of room-temperature frequency-multiplied sources with up to 10x higher output power in the 160-GHz-1.6-THz range, IEEE Trans. Terah. Sci. Technol. 8 (2018) 596–604.

[43] T.W. Crowe, J.L. Hesler, S.A. Retzloff, D.S. Kurtz, Ieee, Higher power multipliers for terahertz sources, 2016 41st International Conference on Infrared, Millimeter, and Terahertz Waves, IEEE, New York, 2016.
[44] J.H. Booske, R.J. Dobbs, C.D. Joye, C.L. Kory, G.R. Neil, G.S. Park, J. Park, R.J. Temkin, Vacuum electronic high power terahertz sources, IEEE Trans. Terah. Sci. Technol. 1 (2011) 54–75.
[45] A.B. Barnes, E.A. Nanni, R.G. Griffin, R.J. Temkin, A 250 GHz gyrotron with a 3 GHz tuning bandwidth for dynamic nuclear polarization, J. Magn. Reson. 221 (2012) 147–153.
[46] A.C. Torrezan, S.T. Han, M.A. Shapiro, J.R. Sirigiri, R.J. Temkin, CW operation of a tunable 330/460 GHz gyrotron for DNP enhanced nuclear magnetic resonance, in: 33rd International Conference on Infrared, Millimeter and Terahertz Waves, Pasadena, CA, 2008, pp. 612–613.
[47] A.C. Torrezan, S.-T. Han, I. Mastovsky, M.A. Shapiro, J.R. Sirigiri, R.J. Temkin, A.B. Barnes, R.G. Griffin, Continuous-wave operation of a frequency tunable 460 GHz second-harmonic gyrotron for enhanced nuclear magnetic resonance, IEEE Trans. Plasma Sci. 38 (2010) 1150–1159.
[48] A.C. Torrezan, M.A. Shapiro, J.R. Sirigiri, R.J. Temkin, R.G. Griffin, Operation of a continuously frequency-tunable second-harmonic CW 330-GHz gyrotron for dynamic nuclear polarization, IEEE Trans. Electron Dev. 58 (2011) 2777–2783.
[49] A. Sodickson, D.G. Cory, Shimming a high-resolution MAS probe, J. Magn. Reson. 128 (1997) 87–91.
[50] F.J. Scott, E.P. Saliba, B.J. Albert, N. Alaniva, E.L. Sesti, C. Gao, N.C. Golota, E.J. Choi, A.P. Jagtap, J.J. Wittmann, M. Eckardt, W. Harneit, B. Corzilius, S.T. Sigurdsson, A.B. Barnes, Frequency-agile gyrotron for electron decoupling and pulsed dynamic nuclear polarization, J. Magn. Reson. 289 (2018) 45–54.
[51] M. Blank, K. Felch, B.G. James, P. Borchand, P. Cahalan, T.S. Chu, H. Jory, B.G. Danly, B. Levush, J.P. Calame, K.T. Nguyen, D.E. Pershing, Development and demonstration of high-average power W-Band gyro-amplifiers for radar applications, IEEE Trans. Plasma Sci. 30 (2002) 865–875.
[52] A.V. Soane, M.A. Shapiro, S. Jawla, R.J. Temkin, Operation of a 140-GHz gyro-amplifier using a dielectric-loaded, severless confocal waveguide, IEEE Trans. Plasma Sci. 45 (2017) 2835–2840.
[53] E.A. Nanni, S.M. Lewis, M.A. Shapiro, R.G. Griffin, R.J. Temkin, Photonic-band-gap traveling-wave gyrotron amplifier, Phys. Rev. Lett. 111 (2013) 235101.
[54] E.A. Nanni, S. Jawla, S.M. Lewis, M.A. Shapiro, R.J. Temkin, Photonic-band-gap gyrotron amplifier with picosecond pulses, Appl. Phys. Lett. 111 (2017) 5.
[55] K. Jaudzems, A. Bertarello, S.R. Chaudhari, A. Pica, D. Cala-De Paepe, E. Barbet-Massin, A.J. Pell, I. Akopjana, S. Kotelovica, D. Gajan, O. Ouari, K. Tars, G. Pintacuda, A. Lesage, Dynamic nuclear polarization-enhanced biomolecular NMR spectroscopy at high magnetic field with fast magic-angle spinning (International ed. in English), Angewa. Chem. 57 (2018) 7458–7462.
[56] P. Fricke, D. Mance, V. Chevelkov, K. Giller, S. Becker, M. Baldus, A. Lange, High resolution observed in 800 MHz DNP spectra of extremely rigid type III secretion needles, J. Biomol. NMR 65 (2016) 121–126.
[57] D.A. Hall, D.C. Maus, G.J. Gerfen, S.J. Inati, L.R. Becerra, F.W. Dahlquist, R.G. Griffin, Polarization-enhanced NMR spectroscopy of biomolecules in frozen solution, Science 276 (1997) 930–932.
[58] Y. Matsuki, K. Ueda, T. Idehara, R. Ikeda, I. Ogawa, S. Nakamura, M. Toda, T. Anai, T. Fujiwara, Helium-cooling and -spinning dynamic nuclear polarization for sensitivity-enhanced solid-state NMR at 14 T and 30 K, J. Magn. Reson. 225 (2012) 1–9.
[59] Y. Matsuki, S. Nakamura, S. Fukui, H. Suematsu, T. Fujiwara, Closed-cycle cold helium magic-angle spinning for sensitivity-enhanced multi-dimensional solid-state NMR, J. Magn. Reson. 259 (2015) 76–81.
[60] D. Lee, E. Bouleau, P. Saint-Bonnet, S. Hediger, G. De Paepe, Ultra-low temperature MAS-DNP, J. Magn. Reson. 264 (2016) 116–124.
[61] A. Purea, C. Reitera, A.I. Dimitriadis, E. Rijk, FabienAussenac, I. Sergeyev, MelanieRosay, FrankEngelke, Improved waveguide coupling for 1.3 mm MAS DNP probes at 263 GHz, J. Magn. Reson. 302 (2019) 43–49.
[62] P.H. Chen, B.J. Albert, C.K. Gao, N. Alaniva, L.E. Price, F.J. Scott, E.P. Saliba, E.L. Sesti, P.T. Judge, E.W. Fisher, A.B. Barnes, Magic angle spinning spheres, Sci. Adv. 4 (2018) 7.
[63] C. Gao, P.T. Judge, E.L. Sesti, L.E. Price, N. Alaniva, E.P. Saliba, B.J. Albert, N.J. Soper, P.-H. Chen, A.B. Barnes, Four millimeter spherical rotors spinning at 28 kHz with double-saddle coils for cross polarization NMR, J. Magn. Reson. 303 (2019) 1–6.
[64] E. Oldfield, R. Norton, A. Allerhand, Studies of individual carbon sites of proteins in solution by natural abundance carbon-13 nuclear magnetic resonance spectroscopy -relaxation behavior*, J. Biol. Chem. 250 (1975) 6368–6380.
[65] G. Morris, R. Freeman, Enhancement of nuclear magnetic resonance signals by polarization transfer, J. Am. Chem. Soc. 101 (1979) 760–762.
[66] A. Henstra, P. Dirksen, J. Schmidt, W.T. Wenckebach, Nuclear spin orientation via electron spin locking (NOVEL), J. Magn. Reson. 77 (1988) 389–393.
[67] A. Henstra, P. Dirksen, W.T. Wenckebach, Enhanced dynamic nuclear polarization by the integrated solid effect, Phys. Lett. A134 (1988) 134.
[68] A. Henstra, W.T. Wenckebach, The theory of nuclear orientation via electron spin locking (NOVEL), Mol. Phys. 106 (2008) 859–871.
[69] T.R. Eichhorn, B. van den Brandt, P. Hautle, A. Henstra, W.T. Wenckebach, Dynamic nuclear polarisation via the integrated solid effect II: experiments on naphthalene-h(8) doped with pentacene-d(14), Mol. Phys. 112 (2014) 1773–1782.
[70] A. Henstra, W.T. Wenckebach, Dynamic nuclear polarisation via the integrated solid effect I: theory, Mol. Phys. 112 (2014) 1761–1772.
[71] T.V. Can, J.J. Walsh, T.M. Swager, R.G. Griffin, Time domain DNP with the NOVEL sequence, J. Chem. Phys. 143 (2015) 054201.
[72] G. Mathies, S. Jain, M. Reese, R.G. Griffin, Pulsed dynamic nuclear polarization with trityl radicals, J. Phys. Chem. Lett. 7 (2016) 111–116.
[73] T.V. Can, R.T. Weber, J.J. Walish, T.M. Swager, R.G. Griffin, Ramped- amplitude NOVEL, J. Chem. Phys. 146 (2017) 7.
[74] S.K. Jain, G. Mathies, R.G. Griffin, Off-resonance NOVEL, J. Chem. Phys. 147 (2017) 13.
[75] T.V. Can, R.T. Weber, J.J. Walish, T.M. Swager, R.G. Griffin, Frequency-Swept Integrated Solid Effect, Angewa. Chem.-Int. Ed. 56 (2017) 6744–6748.
[76] T.V. Can, J.E. McKay, R.T. Weber, C. Yang, T. Dubroca, J. van Tol, S. Hill, R.G. Griffin, Frequency-swept integrated and stretched solid effect dynamic nuclear polarization, J. Phys. Chem. Lett. (2018) 3187–3192.
[77] K.O. Tan, C. Yang, R.T. Weber, G. Mathies, R.G. Griffin, Time-optimized pulsed dynamic nuclear polarization, Sci. Adv. 5 (2019) 7.
[78] E.P. Saliba, E.L. Sesti, N. Alaniva, A.B. Barnes, Pulsed electron decoupling and strategies for time domain dynamic nuclear polarization with magic angle spinning, J. Phys. Chem. Lett. 9 (2018) 5539–5547.